JOURNAL OF VIROLOGY, Apr. 1999, p. 3246–3257 Vol. 73, No. 4
0022-538X/99/$04.00+0

Analysis of the Phosphorylation Sites of Herpes Simplex Virus Type 1 Regulatory Protein ICP27

YAN ZHI AND ROZANNE M. SANDRI-GOLDIN*

Department of Microbiology and Molecular Genetics, University of California, Irvine, California 92697-4025

Received 31 July 1998/Accepted 14 January 1999

The herpes simplex virus type 1 (HSV-1) regulatory protein ICP27 is a 63-kDa phosphoprotein required for viral replication. ICP27 has been shown to contain both stable phosphate groups and phosphate groups that cycle on and off during infection (K. W. Wilcox, A. Kohn, E. Sklyanskaya, and B. Roizman, J. Virol. 33:167–182, 1980). Despite extensive genetic analysis of the ICP27 gene, there is no information available about the sites of the ICP27 molecule that are phosphorylated during viral infection. In this study, we mapped several of the phosphorylation sites of ICP27 following in vivo radiolabeling. Phosphoamino acid analysis showed that serine is the only amino acid that is phosphorylated during infection. Two-dimensional phosphopeptide mapping showed a complex tryptic phosphopeptide pattern with at least four major peptides and several minor peptides. In addition, ICP27 purified from transfected cells yielded a similar phosphopeptide pattern, suggesting that cellular kinases phosphorylate ICP27 during viral infection. In vitro labeling showed that protein kinase A (PKA), PKC, and casein kinase II (CKII) were able to differentially phosphorylate ICP27, resulting in distinct phosphopeptide patterns. The major phosphorylation sites of ICP27 appeared to cluster in the N-terminal portion of the protein, such that a frameshift mutant that encodes amino acids 1 to 163 yielded a phosphopeptide pattern very similar to that seen with the wild-type protein. Further, using small deletion and point mutations in kinase consensus sites, we have elucidated individual serine residues that are phosphorylated in vivo. Specifically, the serine at residue 114 was highly phosphorylated by PKA and the serine residues at positions 16 and 18 serve as targets for CKII phosphorylation in vivo. These kinase consensus site mutants were still capable of complementing the growth of an ICP27-null mutant virus. Interestingly, phosphorylation of the serine at residue 114, which lies within the major nuclear localization signal, appeared to modulate the efficiency of nuclear import of ICP27.

The herpes simplex virus type 1 (HSV-1) regulatory protein ICP27 is a 512-amino-acid, 63-kDa phosphoprotein that localizes to the nuclei of infected cells (1, 22, 50). ICP27 is essential for viral replication (27, 37, 38, 40, 41), and it has been shown to perform some of its regulatory functions at the posttranscriptional level by influencing RNA processing and export (13, 15, 25, 26, 34, 42–45, 47, 49). That is, ICP27 appears to contribute to the shutoff of host protein synthesis by impairing host cell splicing (13, 15), and it has been shown to contribute to the efficient expression of HSV-1 early and late gene products by affecting 3′RNA processing (25, 26) and viral RNA export (36, 42).

Numerous studies have been done to define the regions of ICP27 that are important for its multiple functions. These studies have indicated that the carboxy-terminal half of ICP27 is required for its activation and repression functions (5, 14, 27, 38, 40). Additionally, one study has implicated the acidic amino-terminal portion of ICP27, from amino acids 12 to 63, in the repressor activity (39). The C-terminal zinc finger-like region is required for the ability of ICP27 to interfere with host cell splicing (13, 15) and to associate with and reassort splicing complex proteins (43, 44). Mears et al. (28) have identified a strong nuclear localization signal (NLS) at amino acids 110 to 137. In addition, the sequence between amino acids 141 and 171 contains two arginine-rich regions that contribute to efficient nuclear localization of ICP27 (16). The first of these arginine-rich sequences resembles RGG boxes found in RNA-binding proteins (4, 12, 21, 23). This region has been shown to be necessary for RNA binding by ICP27 both in vitro (29) and in vivo (42). Furthermore, in vivo, the arginine residues in this region are methylated (29). Recently, we (42, 49) and others (30, 35) have demonstrated that ICP27 is one of the nuclear shuttling proteins and that it contains a leucine-rich nuclear export signal (NES) at the amino terminus (42).

ICP27 has been shown to undergo phosphorylation in infected cells (1, 50) and to undergo adenylation and guanylation in isolated nuclei of infected HeLa cells (3). Two species of ICP27 were resolved by sodium dodecyl sulfate-polyacrylamide gel electrophoresis (SDS-PAGE), and as many as five species, heterogeneous only with respect to charge, were resolved by two-dimensional isoelectrofocusing (1, 33). The precise nature of the posttranslational modifications and the origin of this heterogeneity of ICP27 have not been elucidated. Despite the extensive genetic analysis of the ICP27 gene, there is no information about the specific sites of phosphorylation of the ICP27 molecule. Therefore, we have begun to localize the phosphorylation sites of ICP27 by two-dimensional phosphopeptide mapping in order to investigate the possible relationship between phosphorylation and the function of this protein. In this study, we have demonstrated that multiple sites on ICP27 are phosphorylated by different kinases both in vivo and in vitro and that the major phosphorylation sites of ICP27 appear to cluster at the N-terminal portion of the protein. Using kinase consensus site mutations, we have demonstrated that the serine at residue 114 is highly phosphorylated by protein kinase A (PKA) and that the serine residues at positions 16 and 18 are

* Corresponding author. Mailing address: Department of Microbiology and Molecular Genetics, College of Medicine, B240 Medical Sciences I, University of California, Irvine, CA 92697-4025. Phone: (949) 824-7570. Fax: (949) 824-8598. E-mail: RMSANDRI@UCI.EDU.

targets for casein kinase II (CKII). However, mutant proteins containing these phosphorylation site mutations are able to support ICP27 deletion virus growth in complementation assays. We have also shown that PKA consensus site mutant S114A, containing a serine-to-alanine substitution at residue 114, was translocated into the nuclei of transfected cells less efficiently than wild-type protein in competition experiments. This result suggests that phosphorylation of serine residue 114 within the major NLS of ICP27 modulates the efficiency of its nuclear import.

MATERIALS AND METHODS

Cells and viruses. Rabbit skin fibroblast (RSF) cells, which were used for both infections and transfections, and cell line 2-2, which contains the wild-type ICP27 gene, were grown as described previously (14, 46, 47). The HSV-1 wild-type strain KOS 1.1, the ICP27 mutant 27-LacZ (which has an insertion of the *lacZ* gene in the ICP27 locus), and the ICP27 deletion mutant 27-del (from which the ICP27 gene has been completely deleted) were described previously (31, 47, 49).

Recombinant plasmids. Plasmid pSG130B/S, which contains the wild-type ICP27 gene, was described previously (14). The construction and characterization of the ICP27 mutant plasmids ΔNES, H17, D2ΔS5, and S18 have been described previously (14, 16, 42). Plasmids pN6, which encodes a mutant ICP27 with one amino acid substitution and an insertion of 4 amino acids between residues 163 and 164, and pS13, which encodes an ICP27 mutant with an insertion of 4 amino acids between residues 262 and 263, were described previously (14). Plasmids containing these mutations were digested at the *Bam*HI site, at nucleotide 1 (14), and at the *Eco*RI site that occurs in the linker insertion in these mutants. The *Bam*HI-to-*Eco*RI fragment of pN6, containing the 5′ noncoding region and the sequence encoding the N-terminal portion of ICP27 from residues 1 to 163, was joined to the C-terminal portion of mutant S13 from residues 264 to 512. This resulted in a frameshift deletion mutant, termed pN6R, which encodes only the N-terminal portion of ICP27 from residues 1 to 163. The *Hin*fI site in the 5′ noncoding region of ICP27 from plasmid pSG130B/S was first modified by treatment with the Klenow fragment of DNA polymerase and ligation of a *Bgl*II linker. A *Pst*I-to-*Bam*HI fragment from plasmid pCMVβ (Clontech), which contains the human cytomegalovirus (HCMV) enhancer and promoter, was inserted into the *Pst*I and *Bgl*II sites of pSG130B/S. This resulted in a plasmid, pCMV-27, in which ICP27 gene expression was driven by the HCMV promoter. A 34-mer oligonucleotide encoding amino acids MDYKDDDDK (17) was inserted in frame into the *Drd*I site upstream of the translational start site of ICP27. The resulting plasmid, pFlag-ICP27, expresses a FLAG epitope in frame at the amino terminus of the ICP27 protein. pFLAG-ICP27 was sequenced around the site of the insertion.

Site-directed mutagenesis. Mutations were introduced into the ICP27 coding sequence by using a QuikChange site-directed mutagenesis kit (Stratagene). The N-terminal half of ICP27 was cloned into pUC18 and was used as the template for mutagenesis. A serine-to-alanine mutation was introduced at residue 114 of ICP27 by using a pair of 27-mer oligonucleotides, 5′-GCCCGGCGACCGGCTTGCTCCCCCGAG-3′ and 5′-CTCGGGGGAGCAAGCCGGTCGCCGGGC-3′. A small deletion of residues 16 to 18 was introduced by using a pair of 48-mer oligonucleotides, 5′-CTAATTGACCTCGGCCTGGACCTCGATCTGGACGAGGACCCCCCCGAG-3′ and 5′-CTCGGGGGGGTCCTCGTCCAGATCGAGGTCCAGGCCGAGGTCAATTAG-3′, and a small deletion of residues 44 to 46 was introduced by using another pair of 48-mer oligonucleotides, 5′-GAATCGGACAGCAGCGGGGAGTGTGACGAGGACATGGAAGACCCCCAC-3′ and 5′-GTGGGGGTCTTCCATGTCCTCGTCACACTCCCCGCTGCTGTCCGATTC-3′. The specific mutations in ICP27 were verified by DNA sequencing. Subsequently, the N-terminal half of the ICP27 gene containing these mutations was joined with the C-terminal half of the wild-type gene, which resulted in three ICP27 mutants termed S114A, Δ16–18aa, and Δ44–46aa, respectively.

The carboxy-terminal half of ICP27 cloned into M13mp18 was also used as a template for single-stranded site-specific mutagenesis. A serine-to-alanine substitution was introduced at residue 334 by using the 21-mer 5′-TCGGGCCGCAGCACCGCCAA-3′. The same substitution was also introduced at residue 311 by using the 21-mer 5′-CAGACGGGTCGCCTGGGAAAC-3′. The mutations were verified by DNA sequencing. These mutants were first cloned into pUC18, using compatible cloning sites, and then the C-terminal half of the ICP27 gene was joined in frame to the N-terminal half at a *Sal*I site that occurs at amino acid 262, recreating the full-length ICP27 gene. The resulting mutant was termed S311,334A. This mutant was also joined to the N-terminal half of mutant S114A, resulting in a triple-substitution mutant, termed S311,334,114A, in which all three serine residues within the consensus PKA sites found in ICP27 were changed to alanine.

Infection and transfection. Confluent monolayers of RSF cells in 100-mm-diameter plastic culture dishes were infected with HSV-1 wild-type strain KOS at a multiplicity of 10 PFU/cell. Cells were transfected with Lipofectamine reagent (Life Technologies), used at 50 μl/dish, and with plasmid DNA at 10 μg/dish as described previously (43). Twenty-four hours after transfection, the cells were infected with 27-LacZ virus at a multiplicity of 10.

Radiolabeling. RSF cells were routinely labeled in vivo 50 min after infection. Labeling with [^{32}P]orthophosphate (New England Nuclear [NEN]) was carried out, using either 500 μCi/ml for tryptic phosphopeptide mapping or 100 μCi/ml for immunoprecipitation in phosphate-free modified eagle medium (ICN) with 2% fetal calf serum, for 3, 5, or 13 h as indicated in the figure legends. Labeling with [^{35}S]methionine (NEN) was performed, using 50 μCi/ml for immunoprecipitation in methionine-free modified eagle medium (ICN) with 2% fetal calf serum, for 5 h.

Immunoprecipitation and immunoblotting procedures. Infected RSF cells were scraped into cold phosphate-buffer-saline (PBS), and both nuclear and cytoplasmic extracts were prepared as described previously (43). Immunoprecipitation was performed with monoclonal antibodies to ICP27 (H1113 and H1119 [Goodwin Institute]), and the antigen-antibody complexes were separated on SDS-polyacrylamide gels as described previously (43). Electrophoretic transfer of proteins to nitrocellulose membranes was performed with a buffer consisting of 20% methanol–25 mM Tris-190 mM glycine (pH 8.5) at 110 mA overnight. Proteins were visualized by enhanced chemiluminescence (ECL; Amersham Life Sciences), using primary antibodies H1113 and H1119 at a dilution of 1:5,000 and the secondary antibody, an anti-mouse immunoglobulin whole antibody linked to horseradish peroxidase (Amersham Life Sciences), at a dilution of 1:5,000.

Immunofluorescence staining. RSF cells seeded onto coverslips in 24-well dishes were transfected with Lipofectamine reagent (Life Technologies), used at 5 μl/well, and total plasmid DNA at 1 μg/well as described previously (43). At 24 h after transfection, the cells were infected with 27-LacZ virus at a multiplicity of 10 for 50 min and then overlaid with fresh medium for 3 h in the presence of the protein synthesis inhibitor cycloheximide (Sigma) at 100 μg/ml. Subsequently, the cells were washed and their incubation was continued in fresh medium without cycloheximide for another 3 h. Cells were fixed, permeabilized, and stained as described previously (44). An anti-ICP27 monoclonal antibody, H1119 (Goodwin Institute), was used at a dilution of 1:500; and an anti-FLAG monoclonal antibody, M2Ab (Kodak), was used at a dilution of 1:400. Cells were examined with a Nikon UFX-II epifluorescence microscope equipped with a 100× objective lens with a numerical aperture of 1.25 (44).

Dephosphorylation of ICP27 in vitro. Dephosphorylation was carried out on ICP27 that had been bound to protein A-Sepharose beads (Pharmacia). After immunoprecipitation, the antigen-antibody complexes were either directly resuspended into gel loading buffer (125 mM Tris-HCI [pH 6.8], 4% [wt/vol] SDS, 20% glycerol, 10% [vol/vol] 2-mercaptoethanol, 0.01% [wt/vol] bromophenol blue) or incubated with dephosphorylation buffer alone or the same buffer containing 300 U of alkaline phosphatase (AP) (Boehringer Mannheim Corp.) in a total volume of 200 μl. The dephosphorylation buffer contained 50 mM Tris-HCl (pH 8.5), 0.1 mM EDTA, 2 mM dithiothreitol, 20 μg of bovine serum albumin per ml, 40 μg of soybean trypsin inhibitor per ml, 20 μg of aprotinin per ml, 8 μg of leupeptin per ml, and 2 μg of pepstatin A per ml. Reaction mixtures were incubated at 37°C for 45 min, and the reaction was stopped by washing the mixtures three times with 0.5 ml of ice-cold PBS. The reaction products either were resuspended in gel loading buffer and separated by SDS-PAGE or were phosphorylated with exogenous kinases as described below.

In vitro phosphorylation of ICP27 with the PKA catalytic subunit, CKII, and PKC. After dephosphorylation of ICP27 as described above, the protein A-Sepharose beads were resuspended in a total volume of 50 μl containing 10 mM Tris-HCl (pH 7.2), 10 mM $MgCl_2$, 50 mM NaCl, 10 mM dithiothreitol, 0.15 mCi of [γ-^{32}P]ATP (NEN), and 60 U of PKA type I catalytic subunit purified from bovine heart (Sigma Chemical Co.) (52). For phosphorylation with CKII, ICP27 bound to protein A-Sepharose beads was resuspended in a total volume of 50 μl containing 20 mM Tris-HCl (pH 7.5), 50 mM KCl, 10 mM $MgCl_2$, 0.15 mCi of [γ-^{32}P]ATP (NEN), and 2 mU of recombinant CKII from *Escherichia coli* (Boehringer Mannheim Corp.). For phosphorylation with PKC, the protein A-Sepharose beads to which dephosphorylated ICP27 was bound were resuspended in a total volume of 50 μl containing 20 mM HEPES (pH 7.4), 10 mM $MgCl_2$, 1 mM $CaCl_2$, 100 mg of phosphatidylserine per ml, 6 μg of diolein per ml, 0.15 mCi of [γ-^{32}P]ATP (NEN), and 50 U of PKC purified from rat brain (Promega) (52). All reaction mixtures were incubated at 30°C for 30 min, and the reactions were stopped by performing four washes with 0.5 ml of ice-cold PBS. The reaction products were resuspended in gel loading buffer and separated by SDS-PAGE.

Determination of phosphoamino acids. Following immunoprecipitation and resolution on an SDS-polyacrylamide gel, the ICP27 band was identified by autoradiography and excised from the gel. The polypeptide was hydrolyzed in 100 μl of 6 N HCl at 110°C for 60 min. The hydrolysate was then lyophilized and resuspended in 10 μl of pH 1.9 buffer (formic acid [88%]-glacial acetic acid-water, 50:156:1,794 [vol/vol/vol]) containing 1 mg of unlabeled phosphoamino acid markers (phosphoserine, phosphothreonine, and phosphotyrosine [Sigma Chemical Co.]) per ml. The samples were spotted onto a thin-layer cellulose (TLC) plate, and electrophoresis was performed for 20 min at 1,500 V in pH 1.9 buffer for the first dimension and for 16 min at 1,300 V in pH 3.5 buffer (glacial acetic acid-pyridine-water, [100:10:1,890 [vol/vol/vol]) for the second dimension. The positions of nonradioactive phosphoamino acid markers were detected by spraying with 0.25% ninhydrin.

Two-dimensional peptide analysis. Regions of unfixed polyacrylamide gels containing ^{32}P-labeled ICP27 protein were identified by autoradiography and excised. The gel slices were boiled for 5 min in 1 ml of 50 mM ammonium

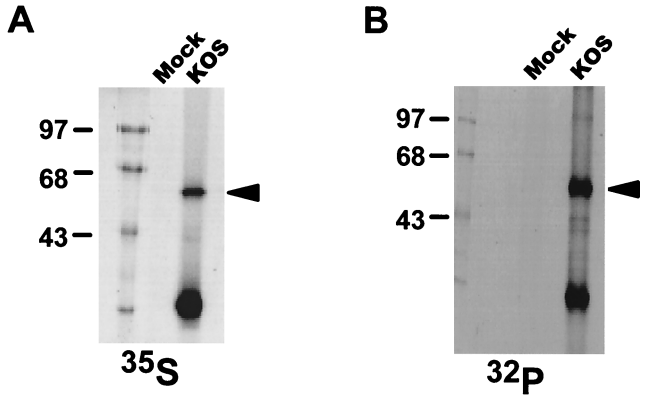

FIG. 1. Immunoprecipitation of [^{35}S]methionine- or $^{32}P_i$-labeled ICP27 from nuclear extracts of HSV-1-infected cells. RSF cells were either mock infected or infected with wild-type HSV-1 strain KOS. Cells were labeled with [^{35}S]methionine (A) or $^{32}P_i$ (B) in vivo for 5 h, after which the cells were harvested and nuclear extracts were prepared. The extracts were immunoprecipitated with anti-ICP27 monoclonal antibodies H1113 and H1119. The antigen-antibody complexes were separated on an SDS-polyacrylamide gel and detected by autoradiography. The bands corresponding to full-length ICP27 are indicated by arrowheads. The positions of protein molecular weight markers are shown on the left (in kilodaltons).

bicarbonate (freshly made) containing 5% 2-mercaptoethanol and 0.1% SDS and then shaken overnight at 37°C. The eluted proteins were precipitated on ice for 4 h by the addition of 250 μl of cold 100% trichloroacetic acid (TCA) in the presence of 20 μg of bovine serum albumin as the carrier protein. The pellet was washed with cold acetone, resuspended in 70 μl of performic acid (freshly made; 9:1 99% formic acid–30% hydrogen peroxide), and oxidized on ice for 1 h. The oxidized protein was diluted with 400 μl of deionized water and then lyophilized. The pellet was resuspended in 70 μl of 50 mM ammonium bicarbonate and was completely digested with 30 μg of tolylsulfonyl phenylalanyl chloromethyl ketone-treated trypsin (Worthington Biochemical Corp.). The digested protein was again lyophilized and washed with deionized water six times. Afterward, the sample was resuspended in 300 μl of pH 4.72 buffer (*n*-butanol–pyridine–glacial acetic acid–water, 100:50:50:800 [vol/vol/vol/vol]) and relyophilized. The peptides were dissolved in 10 μl of pH 4.72 buffer and spotted on TLC plates along with 1.0 μl of tracking dye (a mixture of 5 mg of ε-dinitrophenyllysine and 1 mg of xylene cyanol blue FF per ml). Electrophoresis was performed toward the cathode in pH 4.72 buffer for 25 min at 1,000 V and was followed by ascending chromatography in isobutyric acid buffer (isobutyric acid–*n*-butanol–pyridine–glacial acetic acid–water, 1,250:38:96:58:558 [by volume]). The positions of labeled peptides were determined by autoradiography (51).

Complementation assays. RSF cells grown in six-well dishes were transfected with Lipofectamine reagent (Life Technologies), used at 15 μl/well, and plasmid DNA at 3 μg/well as described previously (43). At 24 h after transfection, the cells were infected with the ICP27 deletion virus 27-del (31) at a final titer of 4×10^6 PFU/well. After adsorption at 37°C for 1 h, the cells were washed with PBS to remove unadsorbed virus. Progeny virus particles were released by three cycles of freezing and thawing 24 h after infection, and the viral titer was determined on 2-2 cells, into which the wild-type ICP27 gene is stably integrated (47).

RESULTS

Phosphoamino acid analysis and phosphopeptide mapping of ICP27 purified from infected cells. It was shown previously that ICP27 contains both stable phosphate groups and phosphate groups that cycle on and off during viral infection (50). However, the sites of ICP27 phosphorylation were not determined. To obtain enough ICP27 to map the phosphorylation sites, we immunoprecipitated this protein from infected cells. RSF cells were either mock infected or infected with wild-type HSV-1 KOS, then labeled with either [^{35}S]methionine (50 μCi/ml) or [^{32}P]orthophosphate (100 μCi/ml) for 5 h. Immunoprecipitations were performed on nuclear extracts, using the ICP27-specific monoclonal antibodies H1113 and H1119. Comparing samples from mock- and KOS-infected cells under both sets of labeling conditions, an abundant band migrating at 63 kDa was seen (Fig. 1). Thus, sufficient full-length ICP27 protein for phosphoamino acid analysis and phosphopeptide mapping could be obtained by excising the band corresponding to ICP27 from SDS-polyacrylamide gels. The lower-molecular-weight protein detected after immunoprecipitation was a major degradation product of ICP27 (see below).

For phosphoamino acid analysis, KOS-infected cells that were labeled with $^{32}P_i$ (500 μCi/ml) beginning 50 min after infection were harvested at 4, 6, and 14 h postinfection. After immunoprecipitation and SDS-PAGE, ICP27 was identified by autoradiography. The protein band was excised, and the protein was eluted and further precipitated with TCA. Phosphoamino acid analysis was performed as described in Materials and Methods. Superimposing the autoradiographs (Fig. 2) onto TLC plates sprayed with ninhydrin showed that serine was the only phosphorylated residue found in the ICP27 polypeptide during viral infection.

Another portion of the TCA-precipitated ICP27 protein derived from the samples harvested at 4, 6, and 14 h after infection was digested to completion with trypsin. The individual peptides were separated by two-dimensional electrophoresis (51). TLC plates were exposed to film. Representative autoradiographs are shown in Fig. 3. Four major spots were consistently observed in independent experiments, and they were designated numerically from 1 to 4. At 4 and 6 h after infection (Fig. 3A and B), spots 2 and 4 were darker than spots 1 and 3. The difference in the intensities of these spots indicated that the stoichiometries and/or the turnover rates of the phosphates at different sites were not equivalent. A diffuse background over spot 1 was always observed. At the later time postinfection (Fig. 3C), the overall phosphorylation level of ICP27 had increased dramatically. The diffuse background around spot 1 became so intense that it eventually covered this spot. Moreover, several minor spots, which were very faint before 6 h postinfection, became more intense and easier to visualize at the later time postinfection. However, the nature of these minor spots is unclear; they could be either partial trypsin digestion products or peptides that contain phosphate groups that cycle on and off during the course of infection (50). Partial-digestion products can be generated when multiple arginine or lysine residues appear in tandem; when a proline, aspartic acid, or glutamic acid residue follows immediately C terminal to an arginine or lysine residue; or when phosphorylated serine residues are present adjacent to the trypsin cleavage site (51). In addition, the material seen at the origin was

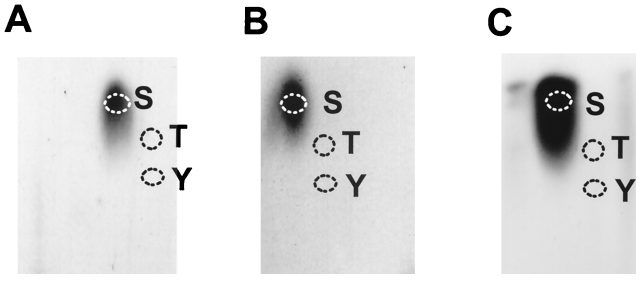

FIG. 2. Phosphoamino acid analysis of ICP27. RSF cells were infected with KOS and labeled with $^{32}P_i$ beginning 50 min after infection. After labeling for 3 h (A), 5 h (B), or 13 h (C), the cells were harvested and nuclear extracts were prepared. ICP27 protein was isolated by immunoprecipitation and fractionation on an SDS-polyacrylamide gel. ICP27 was eluted from gel slices and subjected to HCl hydrolysis. The hydrolysates were analyzed by electrophoresis in pH 1.9 buffer in the first dimension and in pH 3.5 buffer in the second dimension. Unlabeled phosphoamino acid standards were stained with 0.25% ninhydrin, and their positions are labeled as follows: S, phosphoserine; T, phosphothreonine; and Y, phosphotyrosine. Labeled phosphoamino acids were detected by autoradiography with intensifying screens.

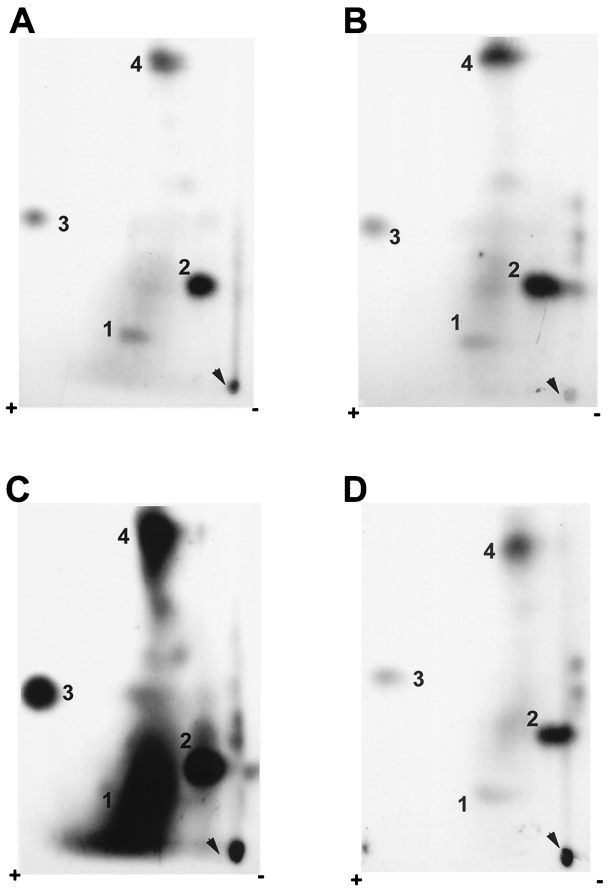

FIG. 3. Two-dimensional tryptic phosphopeptide maps of ICP27 from infected cells labeled in vivo. RSF cells were infected with KOS and labeled with $^{32}P_i$ in vivo beginning 50 min after infection. Immunoprecipitated ICP27 was fractionated on an SDS-polyacrylamide gel, eluted from the gel slice, precipitated with TCA, and then digested to completion with TPCK-treated trypsin. The peptides were dissolved in pH 4.72 buffer. Electrophoresis was performed from the cathode (right) toward the anode (left) in pH 4.72 buffer for 25 min at 1,000 V and was followed by chromatography from bottom to top in isobutyric acid buffer. The positions of labeled peptides were visualized by autoradiography with intensifying screens. ICP27 was immunoprecipitated from nuclear extracts of infected cells labeled in vivo for 3 h (A), 5 h (B), or 13 h (C); it was also immunoprecipitated from the cytoplasmic fraction of infected-cell extracts that were labeled for 5 h (D). Arrowheads indicate the sample origins on the TLC plates. Major phosphopeptides are numbered 1 to 4.

likely derived from undissolved peptides, because in some experiments, when the sample was completely dissolved and separated, no additional spots or streaks were observed in this region.

Even though ICP27 localizes predominantly in the infected-cell nucleus, a detectable amount of protein, which is also phosphorylated, can be seen in the cytoplasm (Fig. 4A and B, lanes 1 and 2), likely due to nuclear export of the protein (42, 49). Therefore, we performed two-dimensional tryptic phosphopeptide mapping on ICP27 immunoprecipitated from cytoplasmic extracts of cells harvested at 6 h (Fig. 3D). The overall level of incorporation of label was less than that seen with the protein from nuclear extracts (Fig. 3B). However, the phosphopeptide pattern was equivalent, including the four major phosphopeptides and a few minor ones. Therefore, nuclear and cytoplasmic ICP27 molecules had very similar, complex phosphorylation patterns during the course of viral infection. It appeared that while the intensity of the phosphorylated peptides increased at later times after infection, phosphorylated sites were similar to those evident early in infection. This is because no new major phosphopeptides were seen. Therefore, tryptic phosphopeptide mapping was routinely performed on ICP27 immunoprecipitated from nuclear extracts of cells harvested at 6 h postinfection. Furthermore, because of the differences in the minor spots, we focused on the four major spots, 1 to 4, in our initial efforts to map the in vivo phosphorylation sites of ICP27.

Phosphopeptide mapping of ICP27 from transfected cells labeled in vivo. At present, three open reading frames (ORFs) in the HSV-1 genome have been shown to be associated with protein kinase activity, including US3, ICP6, encoding the large subunit of ribonucleotide reductase, and UL13. Therefore, it was deemed of interest to determine whether a viral or cellular kinase(s) is mainly responsible for phosphorylation of ICP27. To investigate this, RSF cells were transfected with an ICP27 expression plasmid in which ICP27 was under the control of the HCMV promoter and enhancer. This resulted in high levels of protein expression in the transfected cells in the absence of ICP27-null mutant virus infection. Cells were labeled with [^{32}P]orthophosphate for 5 h beginning 24 h after transfection, after which ICP27 was purified from nuclear extracts by immunoprecipitation and fractionation on an SDS-polyacrylamide gel. The protein was transferred to a nitrocellulose membrane, which was first exposed to film (Fig. 4A, lane 3) and then probed with ICP27 monoclonal antibodies (Fig. 4B, lane 3). It appeared that the expression level of ICP27 from transfected cells was even higher than that from KOS-infected cells (Fig. 4A and B; compare lanes 1 and 3). More importantly, ICP27 was phosphorylated to a similar extent in transfected cells and in virus-infected cells, which indicated that cellular kinases were able to efficiently phosphorylate this protein. To determine if the phosphorylation pattern

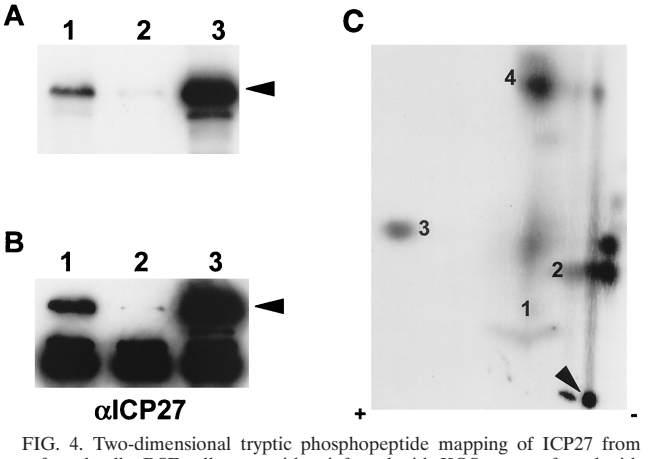

FIG. 4. Two-dimensional tryptic phosphopeptide mapping of ICP27 from transfected cells. RSF cells were either infected with KOS or transfected with plasmid pCMV-ICP27 expressing ICP27 and labeled with $^{32}P_i$ for 5 h. (A and B) Immunoprecipitated ICP27 from either a nuclear extract of infected cells (lanes 1), a cytoplasmic extract of infected cells (lanes 2), or a nuclear extract of transfected cells (lanes 3) was resolved on an SDS-polyacrylamide gel and transferred to a nitrocellulose membrane. The position of ICP27 is indicated by arrowheads. (A) The radioactively labeled proteins on the blot were detected by autoradiography. (B) The blot was subsequently probed with anti-ICP27 monoclonal antibodies (αICP27). The dark band seen in all lanes at 55 kDa is heavy-chain immunoglobulin G which reacts with the secondary antibody used in Western analysis and is present because immunoprecipitated proteins were transferred to the membrane. (C) Immunoprecipitated ICP27 from a nuclear extract of transfected cells (lanes 3, panels A and B) was subjected to two-dimensional tryptic phosphopeptide mapping as described in the legend to Fig. 3. The arrowhead indicates the sample origin on the TLC plate. The four major phosphopeptides are identified by numbers.

in transfected cells was the same as that in infected cells, two-dimensional tryptic phosphopeptide mapping was performed on ICP27 purified from transfected cells (Fig. 4C). By comparing Fig. 4C and 3B, it became apparent that the phosphopeptide pattern of ICP27 expressed from a transfected plasmid was equivalent to that seen with the wild-type protein synthesized during viral infection, in that the same four major spots, as well as a few minor spots, were present. These data strongly suggest that cellular kinases, not viral kinases, phosphorylate ICP27 during viral infection.

In vitro phosphorylation of ICP27 with the PKA catalytic subunit, CKII, and PKC. Little is known about which cellular kinases phosphorylate ICP27 in vivo. However, kinases such as PKA, CKII, and PKC have been implicated in HSV-1 replication (53). Furthermore, there are good consensus sites for PKA, CKII, and PKC phosphorylation in the predicted peptide sequence of ICP27. Therefore, to approach the question of which cellular kinases phosphorylate ICP27 during viral infection, we first studied phosphorylation in vitro, using purified PKA, CKII, and PKC. ICP27 was immunoprecipitated from KOS-infected cells and dephosphorylated with AP to remove phosphate groups that were added in vivo. As seen in Fig. 5A, AP efficiently dephosphorylated ICP27 in vitro in that most of the phosphate was removed from ICP27 by treatment with this enzyme (lane 3). This resulted not only in a significant decrease in the amount of radiolabel present in the sample (compare lanes 1 and 2 with lane 3) but also in a slightly faster rate of migration on an SDS-polyacrylamide gel, consistent with a loss of negatively charged phosphate groups, as seen when the membrane was treated with antibodies to ICP27, as in the Western blot shown on the right (Fig. 5B; compare lanes 1 and 2 with lane 3). These results also clearly indicated that the dephosphorylation conditions used did not cause any significant protein degradation.

After dephosphorylation, ICP27 was phosphorylated in vitro with either purified PKA catalytic subunit, CKII or PKC. When ICP27 was incubated with [γ-^{32}P]ATP in the absence of kinase (Fig. 5C, lanes 2, 4, and 6), there was no detectable incorporation of the ^{32}P label. This result suggested that ICP27-immunoprecipitated complexes did not contain any functional cellular kinase and that ICP27 was not able to phosphorylate itself. PKA, CKII, and PKC were all able to phosphorylate ICP27 in vitro (Fig. 5C, lanes 1, 3, and 5, respectively). Considering the amount of immunoprecipitated ICP27, as measured by Western blot analysis (Fig. 5D), it appeared that PKA phosphorylated ICP27 to the greatest extent and that PKC phosphorylated ICP27 to the least extent. This result was confirmed by tryptic phosphopeptide mapping (see below).

To determine whether phosphorylation of ICP27 by PKA, CKII, or PKC actually occurred at the sites that are used in vivo, we performed two-dimensional phosphopeptide mapping on the in vitro-phosphorylated ICP27 proteins (Fig. 5C). Figure 6 shows the maps of tryptic phosphopeptides of ICP27 that were labeled by incubation with either PKA (Fig. 6A), CKII (Fig. 6B), or PKC (Fig. 6C). The positions of individual phosphopeptides in each case were determined by superimposing the map of in vitro-labeled tryptic peptides with that of in vivo-labeled peptides seen at 14 h after infection (Fig. 3C). Overlapping spots were marked. Because of the higher efficiency of in vitro phosphorylation than of in vivo phosphorylation of ICP27, only the phosphopeptide pattern of the later time point during viral infection could be compared directly with that of in vitro phosphorylation. For ICP27 labeled with PKA (Fig. 6A), three spots corresponded to major spots 1, 2, and 3, which were also observed after labeling in vivo (Fig. 3C). Spot 2 corresponded to the peptide most efficiently labeled by

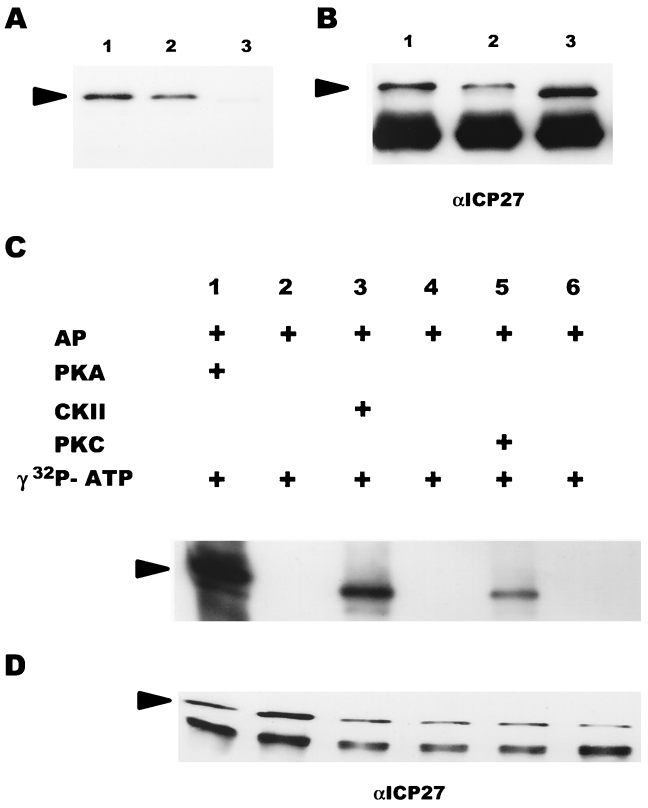

FIG. 5. Dephosphorylation of ICP27 by AP and subsequent in vitro phosphorylation with purified PKA catalytic subunit, CKII, or PKC. (A and B) ICP27 from KOS-infected RSF cells was immunoprecipitated and bound to protein A-Sepharose beads. The antigen-antibody complexes were either directly resuspended into SDS sample buffer (lanes 1), incubated with phosphatase buffer alone (lanes 2), or treated with AP (lanes 3). The reaction products were analyzed on an SDS-polyacrylamide gel and transferred to a nitrocellulose membrane. The blot was first exposed to film (A) and then probed with anti-ICP27 monoclonal antibodies (αICP27) (B). The heavy-chain immunoglobulin G band, as described in the legend to Fig. 4, can be seen in all lanes in panel B. (C and D) Dephosphorylated ICP27 was subsequently subjected to in vitro kinase reactions in the absence of added kinase (lanes 2, 4, and 6) or in the presence (+) of exogenous PKA (lanes 1), CKII (lanes 3), or PKC (lanes 5). The reaction products were analyzed on an SDS-polyacrylamide gel and transferred to a nitrocellulose membrane. The radioactively labeled proteins on the blot were visualized by autoradiography with intensifying screens (C); the blot was subsequently probed with anti-ICP27 monoclonal antibodies (D). The positions of ICP27 are indicated by arrowheads.

PKA. However, upon comparison of Fig. 3C and Fig. 6A, distinct differences were evident. Specifically, several minor spots produced during in vivo phosphorylation became much more prominent when ICP27 was phosphorylated with PKA in vitro. In addition, a few new spots were observed. There are several possible explanations for these observations. First, it is possible that there is a complex balance between phosphorylation and dephosphorylation in vivo and that equilibrium cannot be mimicked in the in vitro kinase reaction. Second, it is possible that several PKA-responsive sites are not easily accessible to kinase in vivo but become available in vitro.

ICP27 labeled in vitro by either CKII or PKC (Fig. 6B and C) produced a subset of the peptides seen in Fig. 3C. Two spots produced by CKII phosphorylation overlapped with major spots 3 and 4 observed in vivo, and in addition, the diffuse background often seen in the region of major spot 1 was observed. Major spot 1 itself was not seen, and this background was seen only in vitro with CKII. Only one spot produced by PKC phosphorylation overlapped with major spot 3 observed

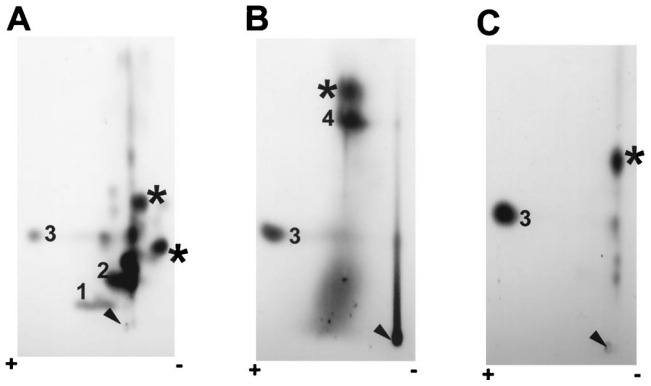

FIG. 6. Two-dimensional phosphopeptide analysis of ICP27 phosphorylated in vitro with purified PKA catalytic subunit, CKII, or PKC. Immunoprecipitated ICP27 from virus-infected cells was first dephosphorylated by AP in vitro, then phosphorylated with PKA (A), CKII (B), or PKC (C) in the presence of [γ-^{32}P] ATP as shown in Fig. 5C, and finally subjected to two-dimensional tryptic phosphopeptide mapping as described in the legend to Fig. 3. Autoradiography was performed with intensifying screens. Arrowheads indicate the sample origins on TLC plates. Major phosphopeptides are identified by numbers, and unique peptides are indicated by asterisks (see the text).

in vivo. There were also some new spots observed in both cases. Thus, in vitro phosphorylation of ICP27 with either PKA, or CKII, or PKC appeared to occur at the in vivo phosphorylation sites. PKA was able to phosphorylate ICP27 at more sites, at least in vitro, than CKII or PKC. More importantly, these results indicated that spots 1 and 2 were mainly derived from PKA phosphorylation, spot 4 and the diffuse background around spot 1 and 2 were mainly derived from PKA phosphorylation, spot 4 and the diffuse background around spot 1 were mainly derived from CKII phosphorylation, and spot 3 might contain sequences recognized by all three kinases.

The major phosphorylation sites of ICP27 are clustered in the N-terminal half of the protein. To begin the mapping of the major phosphopeptides that result from in vivo phosphorylation, we analyzed the phosphorylation of a protein expressed by a frameshift mutant, termed N6R, that encodes ICP27 from amino acids 1 to 163. This was done because a commonly observed major degradation product of ICP27 was labeled to the same or a slightly greater extent than the full-length protein (Fig. 1). This degradation product, which has an apparent molecular size of around 28 kDa, must encode the N-terminal portion of ICP27 because both monoclonal antibodies used for immunoprecipitation recognize epitopes in the N-terminal portion of the protein (28). Because we do not have a recombinant virus containing the N6R mutation, cells were transfected with a plasmid encoding the ICP27 frameshift mutant and, subsequently, the transfected cells were infected with the ICP27-null mutant virus 27-LacZ. Under these conditions, the only ICP27 protein expressed during infection was from the transfected mutant plasmid. Cells were labeled with [^{32}P]orthophosphate for 5 h beginning 50 min after infection, after which ICP27 was purified from nuclear extracts by immunoprecipitation and fractionation on an SDS-polyacrylamide gel. The proteins were transferred to a nitrocellulose membrane, which was first exposed to film (Fig. 7A) and then probed with ICP27 monoclonal antibodies (Fig. 7B). The results suggested that the mutant protein still contained most of the phosphorylation sites, since it was able to incorporate ^{32}P label to a level similar to that incorporated by the wild type. The lower-molecular-weight protein detected in the immunoprecipitation of the wild-type protein (Fig. 7A) represented the major degradation product of ICP27 described above; this was confirmed by Western blotting analysis (Fig. 7B). The origin and biological significance of this degradation product are unknown. Both wild-type and mutant ICP27 were excised from the unfixed SDS-polyacrylamide gel, and tryptic phosphopeptide mapping was performed (Fig. 7C and D). Comparison of Fig. 7C and Fig. 3B showed that the phosphopeptide pattern of wild-type ICP27 expressed from a transfected plasmid and subsequently infected with 27-LacZ was equivalent to that seen with wild-type protein synthesized during viral infection with HSV-1 KOS. The pattern also contained four major spots, a few minor spots, and the diffuse background around spot 1. Interestingly, the frameshift mutant protein reproduced all four major spots and several minor spots as well (Fig. 7D). This indicated that the major phosphorylation sites of ICP27 appear to be clustered in the N-terminal portion of the protein, from amino acids 1 to 163.

Phosphopeptide mapping of mutant ICP27 proteins. To further define the major phosphorylation sites of ICP27, we analyzed the phosphorylation of several mutant proteins containing either point mutations or small deletions within the N-terminal half of ICP27. There are several protein kinase consensus sites within the N-terminal region, including sites for PKA, CKII, and PKC. Since serine is the only phosphorylated residue found in the ICP27 polypeptide during viral infection (Fig. 2), we focused on potential phosphoserine consensus sites. According to the PKA consensus motif RXXS* (32), there is one putative PKA consensus site, at residue 114. A

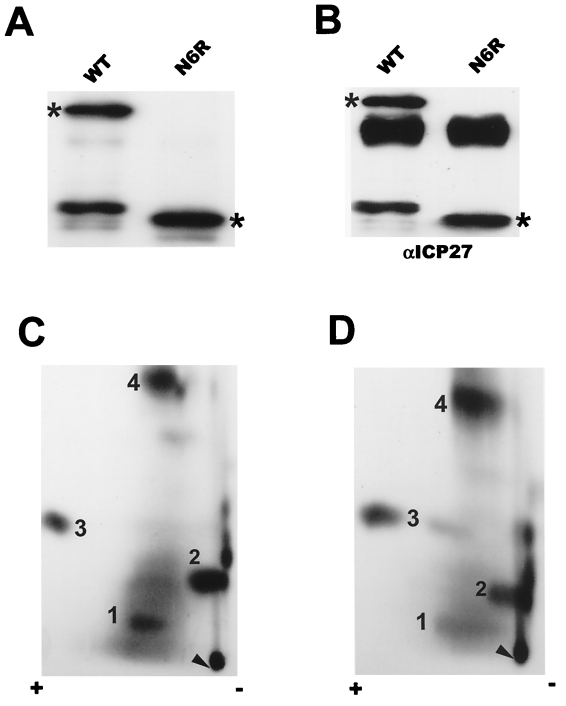

FIG. 7. Phosphorylation of wild-type ICP27 and frameshift mutant N6R in vivo. RSF cells were transfected with plasmids encoding either wild-type (WT) ICP27 or the frameshift mutant N6R. Twenty-four hours later, the cells were infected with 27-LacZ. Labeling with $^{32}P_i$ was done for 5 h beginning 50 min after infection. ICP27 proteins were immunoprecipitated with anti-ICP27 monoclonal antibodies (αICP27), separated by SDS-PAGE, and transferred to a nitrocellulose membrane. The blot was first exposed to film (A) and then probed with anti-ICP27 monoclonal antibodies (B). The bands corresponding to full-length ICP27 and to mutant ICP27 are indicated by asterisks. (C and D) Phosphopeptides of both wild-type ICP27 (C) and frameshift mutant N6R, encoding ICP27 from amino acids 1 to 163, were generated by treatment with trypsin and resolved on TLC plates as described in the legend to Fig. 3. Major phosphopeptides are identified by numbers.

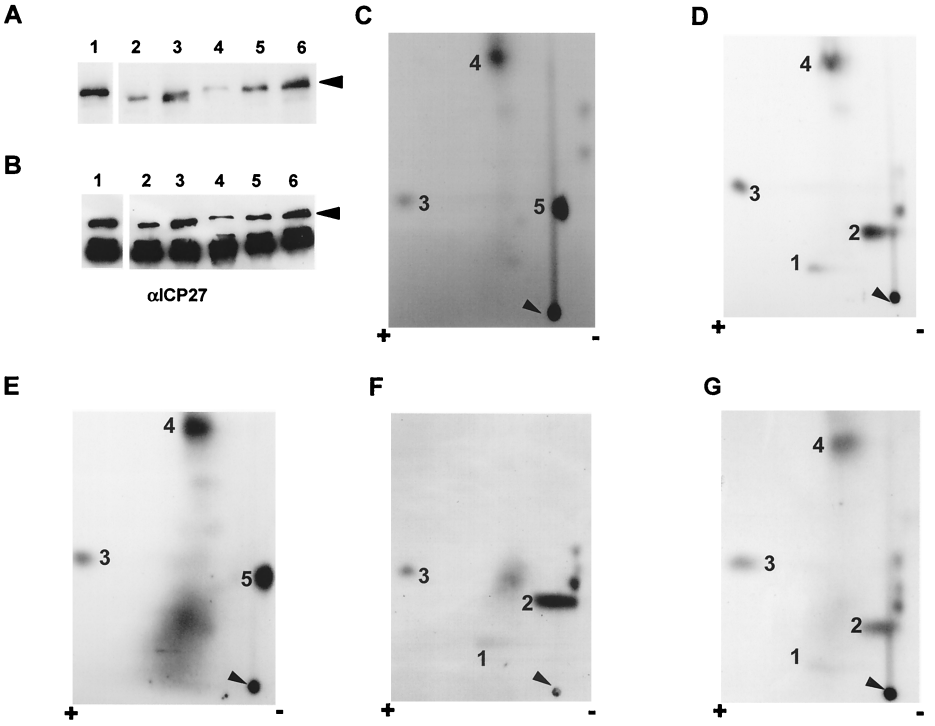

FIG. 8. Phosphopeptide analysis of ICP27 mutant proteins labeled in vivo. RSF cells were transfected with a series of phosphorylation site-specific mutants. Viral infection with 27-LacZ to boost protein expression, in vivo $^{32}P_i$ labeling, and immunoprecipitation of ICP27 were performed as described in the legend to Fig. 7. ICP27 proteins were separated by SDS-PAGE and transferred to a nitrocellulose membrane. (A and B) The blot was first exposed to film (A) and then probed with anti-ICP27 monoclonal antibodies (αICP27) (B). Lanes: 1, wild-type ICP27; 2, CKII consensus site mutant Δ16–18aa, from which residues 16 to 18 were deleted; 3, CKII consensus site mutant Δ44–46aa, from which residues 44 to and 46 have been deleted; 4, PKA consensus site single-mutant S114A, containing a serine-to-alanine substitution at residue 114; 5, PKA consensus site double-mutant S311,334A, containing serine-to-alanine substitutions at residues 311 and 334; 6, PKA consensus site triple-mutant S114,311,334A, containing serine-to-alanine substitutions at residues 114, 311, and 334. The position of ICP27 is indicated by arrowheads. (C to G) Phosphopeptides of each mutant ICP27 protein were generated by treatment with trypsin and resolved on TLC plates as described in the legend to Fig. 3. Arrowheads indicate the sample origins. Major phosphopeptides are identified by numbers. (C) S114A; (D) S311,334A; (E) S114,311,334A; (F) Δ16–18aa; (G) Δ44–46aa.

PKA consensus site mutant termed S114A, which contains a serine-to-alanine substitution at residue 114, was generated by site-directed mutagenesis. Cells were transfected with this mutant construct, and tryptic phosphopeptide mapping was performed as described earlier. Overall, the ^{32}P-labeled peptide recovery rate for this mutant was much lower than that for the wild type (Fig. 8A; compare lanes 1 and 4). However, focusing on the major spots in the phosphopeptide map, it can be seen that mutant S114A yielded a peptide pattern different from that of wild-type ICP27 (Fig. 8C). Specifically, two of the major peptides, 1 and 2, were not detected and one minor peptide, designated as 5, became more predominant. Peptides 1, 2, and 5 lay on a diagonal sloping toward the anode, which suggested that these peptides might be phosphoisomers, with peptide 5 being the least-phosphorylated form and peptide 1 being the most highly phosphorylated form. This result suggested that the serine at residue 114 was highly phosphorylated by PKA in vivo and that this serine residue might have adverse effects on the phosphorylation of one or more nearby serine residues. This is because a mutation at this single site caused the most highly phosphorylated isomer, major peptide 1, to disappear and the least-phosphorylated isomer, peptide 5, to become more predominant. To verify this result, the same mutant construct was transfected into cells and the mutant ICP27 protein, purified by immunoprecipitation, was subsequently dephosphorylated prior to being rephosphorylated in vitro with PKA. After PKA phosphorylation in vitro, the mutant protein was analyzed by tryptic phosphopeptide mapping. The major spots, 1 and 2, were also missing, and minor spot 5 was very distinct (data not shown). Since spot 2 was one of the peptides most efficiently labeled by PKA (Fig. 6A), this result further supported the conclusions that the serine at position 114 was phosphorylated in vivo by PKA and that it was phosphorylated in a majority of the ICP27 molecules in the nuclei of infected cells. As a further test of this conclusion, we performed phosphopeptide mapping on two additional PKA consensus site mutants following in vivo labeling as outlined above. Mutant S311,334A has two amino acid substitutions; the serine residues that occur in two consensus PKA sites, at residues 311 and 334, were replaced by alanine residues. The phosphopeptide pattern of this mutant protein (Fig. 8D) was equivalent to that of wild-type ICP27 (Fig. 7C). The four major spots were clearly seen. Since both of these PKA sites occur in the C-terminal half of ICP27, this result supports the conclusion that the major phosphorylation sites of ICP27 that are phosphorylated during infection occur in the N-terminal portion of the protein. This can be further seen with the triple PKA consensus site mutant, S114,311,334A, in which the serine residues at positions 114, 311, and 334 have all been replaced by alanine. In this case, the phosphopeptide map derived from the mutant protein labeled in vivo was very similar to that seen with the single-mutant S114A (compare Fig. 8E and C). Major spot 1 was barely detectable over the diffuse background around spot 1. Further, spot 2 was not found and minor spot 5 was very prominent (Fig. 8E). This was the pattern seen with mutant S114A (Fig. 8C), indicating that, in vivo, only the serine at position 114 is phosphorylated and that the serines at 311 and

334 are not phosphorylated despite their positions in PKA consensus sites.

There are two putative CKII consensus sites, at residues 16 and 18, based on the CKII phosphorylation site motif S*XX (D/E) (32). Therefore, we analyzed the phosphorylation pattern of a small-deletion mutant, Δ16–18aa, from which residues 16 to 18 have been deleted. In the tryptic phosphopeptide map of this mutant protein labeled in vivo (Fig. 8F), the most distinct difference from the wild-type map, as seen in Fig. 7C, was that the deletion mutant protein did not produce major peptide 4. Since peptide 4 was one of the major spots seen when ICP27 was phosphorylated with CKII in vitro (Fig. 6B), this result indicates that either one or both of the CKII consensus serine residues was phosphorylated in vivo. To differentiate between these two possibilities, two additional single CKII consensus site mutants, termed S16A and S18A, which contain a serine-to-alanine substitution at residues 16 and 18, respectively, were also generated by site-directed mutagenesis. Tryptic phosphopeptide mapping was performed with these mutant constructs as described above. It appeared that both mutant proteins, like the wild type, were able to produce major peptide 4 (data not shown). This result suggests that both serine 16 and serine 18 are phosphorylated by CKII in vivo. However, we cannot rule out the possibility that these two serine residues are redundant with regard to phosphorylation by CKII in vivo.

Computer alignment of protein sequences of ICP27 homologues from several herpesviruses revealed that there are conserved consensus CKII sites near the N termini of HSV-1 and HSV-2 ICP27, Epstein-Barr virus (EBV) SM protein, and herpesvirus saimiri ORF 57 (8). Specifically, there are three putative CKII consensus sites at serine residues 44, 45, and 46 in HSV-1 ICP27. However, deletion of these consensus CKII sites did not reduce the in vitro phosphorylation of ICP27 by CKII (data not shown). Furthermore, deletion mutant Δ44–46aa was still able to produce all four major spots and a few minor spots seen with the wild-type protein, when labeled in vivo (Fig. 8G). These results suggest that these serine residues are not highly phosphorylated either in vivo or in vitro. However, we cannot rule out the possibility that nearby serine residues were able to be phosphorylated by CKII when the conserved serine residues were absent.

It should be noted that the levels of recovery of ^{32}P-labeled peptides from some of the mutant proteins, especially S114A, were somehow lower than that of the wild type. To demonstrate the levels of phosphorylation and protein expression for each mutant compared to the wild type, mutant and wild-type proteins were purified as described previously, the nitrocellulose membrane was exposed to film (Fig. 8A), and then the membrane was probed with anti-ICP27 monoclonal antibodies (Fig. 8B). The lower level of phosphorylation observed in S114A (lane 4) was partially due to a lower level of protein expression compared to that of the wild type (lane 1). However, the overall protein expression levels of the other mutants were comparable to that of wild-type ICP27. Importantly, the triple PKA site mutant protein S114,311,334A (lane 6) was expressed at a level similar to that of the wild type (lane 1), yet its tryptic phosphopeptide map (Fig. 8E) was the same as that seen with mutant S114A (Fig. 8C). This indicates that the observed phosphopeptide pattern was not influenced by the level of protein expression.

ICP27 kinase consensus site mutants were able to support ICP27 deletion virus growth. To determine if phosphorylation plays an essential role in ICP27 function, we investigated the ability of the protein kinase consensus site mutants to support viral infection in complementation assays. RSF cells were transfected with each of the mutant ICP27 constructs, as indicated in Table 1, or with wild-type ICP27 or pGEM-1 vector alone. Twenty-four hours after transfection, the cells were infected with an ICP27 deletion virus, 27-del. Twenty-four hours later, viral progeny were assayed on the complementing cell line 2-2 (48) (Table 1). In this assay, pGEM-1 served as a negative control, and its ability to support 27-del virus growth was arbitrarily set to an index value of 1. Wild-type ICP27 (pSG130B/S) served as a positive control and yielded viral-progeny titers either 20- or 14-fold higher than those seen with pGEM-1 alone in two independent experiments. Since viral yields from transfected cells differed, possibly due to the transfection efficiency, we compared the complementation indices rather than the viral-progeny titers of different experiments. ICP27 is essential for viral replication (24, 40, 41, 47), and mutations introduced into important functional regions of this protein result in defective proteins that are not able to complement 27-del. Three well-defined ICP27 mutants, including a nuclear export mutant (ΔNES [42]), a nuclear localization mutant (D2ΔS5 [16]), and an activator mutant (H17 [14]), all failed to support 27-del virus growth. However, the PKA consensus site mutant S114A and the two CKII consensus site mutants, Δ16–18aa and Δ44–46aa, were all capable of complementing 27-del growth, although to somewhat lesser extents than the wild type. Both S114A and Δ16–18aa did show some defects in phosphorylation in vivo, as determined by tryptic phosphopeptide mapping. Since complementation assays can only detect dramatic defects in ICP27 activities, and not subtle ones, we cannot determine whether the slight differences seen in Table 1 among the protein kinase consensus site mutants are biologically significant.

TABLE 1. Ability of ICP27 kinase consensus site mutants to complement ICP27 deletion virus growth[a]

Plasmid	Viral yield (PFU)		Complementation index[b]	
	Expt 1	Expt 2	Expt 1	Expt 2
pGEM	1.0×10^4	4.1×10^5	1	1
Wild-type ICP27	2.0×10^5	5.9×10^6	20	14.3
ΔNES	4.0×10^4		4	
Δ16–18aa	1.5×10^5		15	
Δ44–46aa	1.5×10^5		15	
D2ΔS5		5.0×10^5		1.2
H17		2.8×10^5		0.7
S114A		2.9×10^6		7.1

[a] RSF cells were transfected with different ICP27 mutant constructs individually as indicated and then infected with an ICP27 deletion virus. The progeny viruses were assayed on the ICP27-complementing cell line 2-2. Average values of two separate transfections for each plasmid are shown.

[b] pGEM-1 vector served as a negative control; its ability to support ICP27 deletion virus growth is arbitrarily defined as an index value of 1. The growth complementation indices of ICP27 mutants were equal to the ratio of the yield of ICP27 deletion virus in RSF cells transfected with a mutant plasmid to the yield in RSF cells transfected with pGEM-1.

Phosphorylation may regulate the efficiency of nuclear import of ICP27. It has been shown that phosphorylation plays an important role in regulating nuclear transport of proteins in eukaryotic cells. The PKA-phosphorylated serine at residue 114 occurs within the major NLS of ICP27 (28). Therefore, to determine whether phosphorylation affects ICP27 nuclear import, mutant S114A was transfected alone or in the presence of different amounts of a wild-type-ICP27-expressing plasmid, pFLAG-ICP27 (54). The wild-type construct contains a synthetic FLAG epitope at the extreme N terminus so that it can be distinguished from the mutant protein, which reacts with

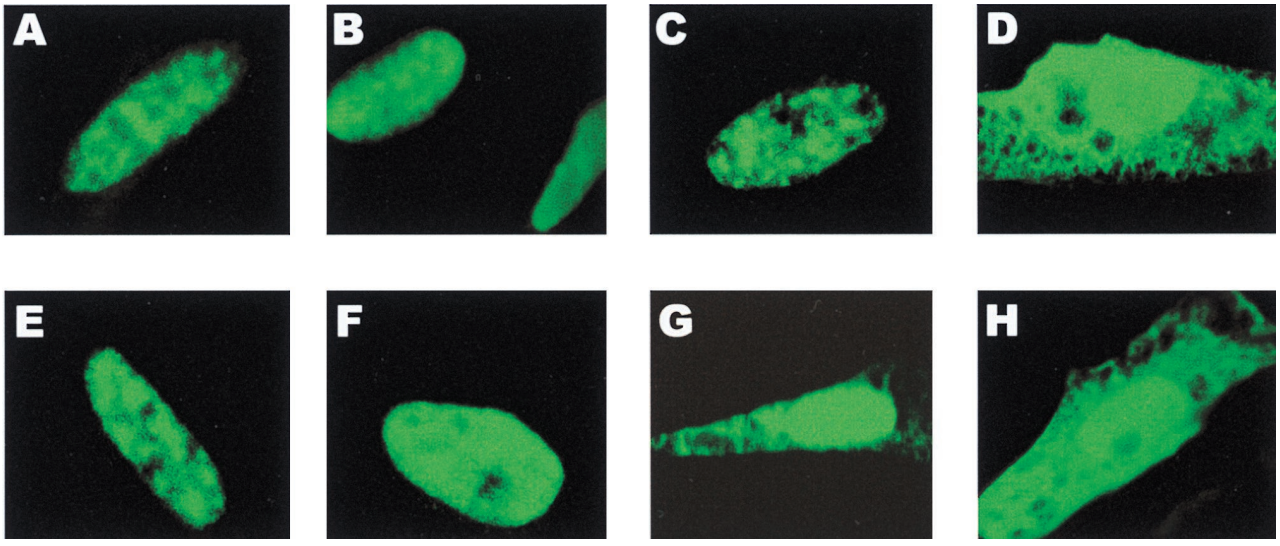

FIG. 9. A serine-to-alanine substitution in the PKA consensus site at residue 114 within the ICP27 NLS results in less-efficient nuclear import of the mutant protein. Cells were transfected with plasmids expressing FLAG epitope-tagged wild-type ICP27 (A) or mutant S311,334A (B), S114A (C), or D2ΔS5 (D). In addition, cells were transfected with S114A plasmid DNA and FLAG-tagged wild-type plasmid at a 5:1 ratio (E), with S311,334A plasmid and the wild-type plasmid at a 5:1 ratio (F), or with FLAG-tagged wild-type plasmid DNA and S114A plasmid at a 5:1 ratio (G and H). Twenty-four hours after transfection, the cells were infected with 27-LacZ virus in the presence of cycloheximide (100 μg/ml). The cells were incubated in the presence of cycloheximide for 3 h, at which time the cells were washed, fresh medium without cycloheximide was added, and incubation was continued for an additional 3 h, after which the cells were fixed. The treatment with cycloheximide was performed to synchronize the boost of protein expression that occurred following infection with the 27-LacZ virus and thus allow monitoring of protein import. Cells were stained with anti-FLAG monoclonal antibody (A and E) or with anti-ICP27 monoclonal antibody H1119 (B to D and F to H).

the anti-ICP27 monoclonal antibody H1119 but not the anti-FLAG monoclonal antibody M2. The FLAG epitope-tagged wild-type ICP27 does not react with H1119, because the position of the FLAG epitope masks the H1119-specific epitope, which also resides at the extreme N terminus. Wild-type ICP27 was found to be exclusively nuclear, as was mutant S114A when transfected into cells alone (Fig. 9A and C, respectively). However, when five times the amount of wild-type ICP27 plasmid DNA was cotransfected with mutant S114A, there was a decrease in the efficiency of nuclear import of this mutant. About 50% of the cells showed a pronounced cytoplasmic fluorescence (Fig. 9G and H), and many of these cells had a nuclear-cytoplasmic fluorescence pattern that was indistinguishable from that seen with mutant D2ΔS5 (Fig. 9D), from which the major NLS has been deleted (16). While wild-type ICP27 could compete with S114A, the converse was not the case, as expected. Adding S114A plasmid DNA to that of the wild type at a 5:1 ratio did not affect the nuclear import of wild-type ICP27 (Fig. 9E). Furthermore, the PKA site mutant S311,334A was found to be exclusively nuclear when transfected alone (Fig. 9B) or with wild-type plasmid DNA at a 5:1 ratio (Fig. 9F). Therefore, these results suggested that phosphorylation of the serine at residue 114 may modulate the efficiency of nuclear import.

DISCUSSION

ICP27 is an essential immediate-early regulatory protein that has been shown to be required for viral inhibition of RNA splicing (15), for activation of the expression of genes containing specific 3′ processing signals (5, 26, 45), and for nuclear export of viral intronless transcripts (36, 42). ICP27 has been shown to be modified posttranslationally by the addition of phosphate groups (50); however, despite extensive genetic analysis of the ICP27 gene, until now there has been no information about the sites of the ICP27 molecule that are phosphorylated during viral infection or about the role that phosphorylation might play in the activities of this protein. Therefore, we have examined the tryptic phosphopeptide patterns of wild-type and mutant ICP27 proteins as a first step toward understanding ICP27 phosphorylation and how phosphorylation at these sites affects the functions of this protein. Serine was found to be the only residue phosphorylated during viral infection. A complex pattern of phosphopeptides, which contained four major spots and a few minor spots, was observed for ICP27 purified from nuclear extracts of infected cells (Fig. 3). We also determined the phosphopeptide pattern of the cytoplasmic form of ICP27, and a very similar pattern was seen (Fig. 3D). Some of the phosphopeptides appeared to be structurally related—for example, major spots 1, 2, and 5. During the course of viral infection, the presence of the major peptides was consistent while that of the minor spots was variable in different experiments and at different times after infection. The origin of these minor spots is currently unknown. They may have resulted from partial digestion by trypsin, from peptides containing unstable phosphate groups, or from peptides that were differentially phosphorylated during viral infection.

Even though there is no evidence to indicate that ICP27 is phosphorylated by any of the known viral kinases, we investigated whether this protein was phosphorylated by a viral or cellular kinase(s) in vivo. When cells were transfected with an expression construct in the absence of viral infection, a phosphopeptide pattern very similar to that seen for ICP27 expressed during viral infection was produced. This result suggests either that cellular kinases are the only kinases that can phosphorylate ICP27 or that both cellular and viral kinases are able to phosphorylate this protein at similar sites in vivo. We favor the first explanation, since it has been shown that viral kinases possess some unique catalytic properties different from those of cellular kinases (7, 9–11). Therefore, we investigated the phosphorylation of ICP27 by three major cellular kinases, PKA, PKC, and CKII. Both PKA and CKII phosphorylated ICP27 to a higher level than PKC in vitro, and ICP27 labeled with PKA, CKII, or PKC yielded different tryptic phosphopep-

tide patterns. Specifically, some, but not all, of the four major spots were produced after labeling with any one of the three kinases (Fig. 6). In addition, a few unique spots which are not readily observed with ICP27 labeled in infected cells were produced in each case. These unique peptides may contain kinase-responsive sites that are not easily accessible to the cognate kinase in vivo but become available in vitro, perhaps because of folding differences or lack of interaction with other cellular or viral proteins that might mask specific sites. These data suggest that PKA and CKII may be the two major protein kinases that are responsible for the phosphorylation of ICP27 in vivo. Interestingly, there were more spots from ICP27 phosphorylated by PKA than from ICP27 phosphorylated by CKII in vitro. Some of these spots corresponded to the minor spots observed with ICP27 labeled in vivo. This suggests that ICP27 may contain a larger number of potential PKA-responsive sites than is apparent based on the defined consensus for PKA sites (32). It is of note that at least two consensus PKA sites—namely, the serine residues at positions 311 and 334—were not phosphorylated in vivo. Additionally, a diffuse background over major spot 1 was observed clearly with ICP27 labeled in infected cells and with wild-type ICP27 phosphorylated by CKII, but not by PKA or PKC, in vitro. This suggests that this diffuse background may reflect the stage of ICP27 phosphorylation by CKII. Importantly, these studies showed that unlike ICP4 (52), immunoprecipitated ICP27 could not undergo phosphorylation without an exogenous kinase, suggesting that ICP27 cannot autophosphorylate.

In our efforts to map the phosphorylation sites of ICP27 in vivo by using frameshift mutant N6R, we were surprised to find that this mutant, which encodes ICP27 from amino acids 1 to 163, was phosphorylated as efficiently as the wild-type protein in vivo. Furthermore, a tryptic phosphopeptide pattern very similar to that for the wild type was seen, including all four major spots and a few minor spots. This indicated that the major phosphorylation sites of ICP27 are located in the N-terminal portion of the protein. For finer mapping, point mutants and two small-deletion mutants were constructed so that specific sites could be pinpointed. It was found that the serine residue at position 114 in the N-terminal portion of ICP27 is highly phosphorylated in vivo. In addition, the serine residues at positions 16 and 18 are likely to be targets for CKII phosphorylation in vivo. A stretch of three CKII consensus serines in the N terminus of ICP27 is highly conserved in other homologues, including EBV SM protein, herpesvirus saimiri ORF 57, and HSV-2 ICP27. Site-directed mutagenesis of these consensus CKII sites in EBV SM greatly reduced the in vitro phosphorylation of SM by CKII, even though this phosphorylation event did not affect the ability of SM to upregulate chloramphenicol acetyltransferase expression in a transient-transfection assay (8). In contrast, ICP27 mutant Δ44–46aa, from which these consensus serine residues were deleted, was efficiently phosphorylated by CKII in vitro and had a tryptic phosphopeptide pattern similar to that of the wild-type protein when labeling was performed in vivo (Fig. 8G). Thus, although these sites are conserved, their phosphorylation does not appear to be critical for protein function.

It is interesting that the major phosphorylation sites of ICP27 that are highly phosphorylated in vivo are located in the amino-terminal portion of the protein, since the C-terminal half of the protein has been shown to be important for both activation and splicing repressor functions (14, 27, 37, 38). Because ICP27 has recently been shown to shuttle between the nucleus and the cytoplasm (30, 35, 42, 49), we considered the possibility that there may exist a subpopulation of ICP27 in which the C-terminal sites are phosphorylated, perhaps in the cytoplasmic fraction. However, ICP27 purified from the cytoplasm yielded the same pattern as nuclear material. It was also possible that the phosphorylation could occur transiently, with the phosphate groups cycling off. To directly study the C-terminal portion of ICP27 to determine whether phosphorylation could be detected, large-deletion mutant R9ΔS13, from which residues 28 to 262 were deleted, was generated (54). Attempts to immunoprecipitate the mutant protein from ^{32}P-labeled whole-cell extracts by using polyclonal antibodies generated against the C-terminal portion of ICP27 were unsuccessful in that we were unable to observe any distinct band around 40 kDa even after long exposure periods (55). Furthermore, the expression of the mutant protein was barely detectable by Western analysis or immunoprecipitation of [^{35}S]methionine-labeled proteins (54). Therefore, the inability to detect the ^{32}P-labeled mutant protein may have been due to a lack of phosphorylation in this region, the extremely low level of expression of the protein, or the rapid turnover of a protein encoding only the C-terminal half of ICP27.

It is also possible that phosphorylation at sites in the C-terminal half of ICP27 targets the protein for early degradation, similar to the situation that occurs with IκBα. The transcription factor NF-κB is sequestered in the cytoplasm by the inhibitor protein IκBα. Extracellular inducers of NF-κB activate signal transduction pathways that result in the phosphorylation of serine residues 32 and 36 of IκBα, and this phosphorylation event targets IκBα to the ubiquitin-proteasome pathway (6). It is interesting to postulate that the phosphorylation of C-terminal sites of ICP27 targets the protein for immediate degradation. A major truncated product of ICP27 that contains only the N-terminal portion of the protein is often seen in the immunoprecipitated complex (Fig. 1). Although there is no available information on the potential function or significance of this product, two lines of evidence suggest that this truncation is not an artifact that occurs because of proteolytic degradation during the preparation of nuclear extracts. First, this product was also found on Western blots from either transfected or infected cells that were directly harvested into SDS sample buffer. Second, it has been reported that glutathione *S*-transferase–ICP27 fusion proteins purified from bacterial-cell lysates contain an N-terminally truncated protein as the major product (29). Interestingly, this was also the case when ICP27 was expressed as a fusion protein in the ThioFusion expression system (55). Thus, this product appears to be generated in vivo in both mammalian and bacterial cells. However, we consider it unlikely that this product arises from proteosome targeting following phosphorylation of the sites in the C-terminal portion of ICP27. First, if that were the case, complete degradation would be expected to occur. Second, pulse-chase experiments using [^{35}S]methionine labeling showed that the half-lives of both nuclear and cytoplasmic ICP27 molecules from KOS-infected cells were at least 5 h, and there were no significant differences in the half-life of mutant N6R, which encodes amino acids 1 to 163, or S311,334A, in which alanines were substituted for the serine residues in two C-terminal PKA sites (55). Both of these mutant proteins might be expected to be more stable than the wild-type protein if C-terminal phosphorylation was a signal for degradation.

The role of ICP27 phosphorylation at the kinase consensus sites that we have mapped has been investigated by two different approaches. Complementation experiments demonstrated that the PKA and CKII consensus site mutants were able to support the growth of an ICP27 deletion mutant only slightly less efficiently than wild-type protein. It is certainly possible that phosphorylation plays a more significant role at different stages of the HSV life cycle in the host. For example, we have

not tested the ability of these mutants to support the growth of an ICP27-null mutant virus in cells of neuronal origin. Recently, it has been shown that deletion of a highly conserved polyserine tract found between residues 184 and 198 in HSV-1 ICP4 results in a virus that is marginally impaired for growth in culture and in the eyes of infected mice but is completely impaired for growth in the trigeminal ganglia (2, 53). To address questions on specific functions and interactions of ICP27 during viral infection, the kinase consensus site mutations are being introduced into the viral genome by marker transfer. Viral growth defects as well as effects on specific functions, such as RNA processing and export, will be analyzed in different cell lines.

By the second approach, we were able to discern a role for the phosphorylation of serine 114, which occurs within the major NLS of ICP27 (28). Recent studies indicate that NLS function can be precisely regulated, with phosphorylation being the main mechanism controlling NLS-dependent nuclear import of a number of proteins (18–20). For example, nuclear localization of the archetypal NLS-containing simian virus large tumor antigen (T-ag) is regulated by the CcN motif, which comprises the T-ag NLS. In this motif, a CKII site (C) 13 amino acids N terminal to the NLS modulates the rate of nuclear import and a cyclin-dependent kinase site (c) adjacent to the NLS regulates the maximal level of nuclear accumulation (19, 20). We examined whether phosphorylation at serine residue 114, which is within the major NLS of ICP27 (residues 110 to 137), had any effect on nuclear import. When transfected into cells alone, mutant S114A was found to be exclusively nuclear; however, in competition experiments with wild-type ICP27, there was a pronounced decrease in the efficiency of nuclear import of this mutant. These data argue that phosphorylation at serine residue 114 modulates the efficiency of ICP27 nuclear import. Biochemical studies to determine which step of nuclear transport is affected by phosphorylation are under way.

In summary, the data presented here represent the first step toward elucidation of the functional roles of ICP27 phosphorylation. Further efforts to map the phosphorylation sites in more detail and to delineate the biological significance of ICP27 phosphorylation may provide some important insights into the multiple functions of this protein.

ACKNOWLEDGMENTS

We thank Saul Silverstein (Columbia University) for the 27-del virus.

This work was supported by Public Health Service grant AI21515 from the National Institute of Allergy and Infectious Diseases to R.M.S.-G.

REFERENCES

1. **Ackermann, M., D. K. Braun, L. Pereira, and B. Roizman.** 1984. Characterization of herpes simplex virus 1 α proteins 0, 4, and 27 with monoclonal antibodies. J. Virol. **52:**108–118.
2. **Bates, P. A., and N. A. DeLuca.** 1998. The polyserine tract of herpes simplex virus ICP4 is required for normal viral gene expression and growth in murine trigeminal ganglia. J. Virol. **72:**7115–7124.
3. **Blaho, J. A., C. Mitchell, and B. Roizman.** 1993. Guanylylation and adenylylation of the α regulatory proteins of herpes simplex virus require a viral β or γ function. J. Virol. **67:**3891–3900.
4. **Burd, C. G., and G. Dreyfuss.** 1994. Conserved structures and diversity of functions of RNA-binding proteins. Science **265:**615–620.
5. **Chapman, C. J., J. D. Harris, M. A. Hardwicke, R. M. Sandri-Goldin, M. K. L. Collins, and D. S. Latchman.** 1992. Promoter independent activation of heterologous gene expression by the herpes simplex virus immediate-early protein ICP27. Virology **186:**573–578.
6. **Chen, Z., J. Hagler, V. J. Palombella, F. Melandri, D. Scherer, D. Ballard, and T. Maniatis.** 1995. Signal-induced site-specific phosphorylation targets IκBα to the ubiquitin-proteasome pathway. Genes Dev. **9:**1586–1597.
7. **Chung, T. D., J. P. Wymer, C. C. Smith, M. Kulka, and L. Aurelian.** 1989. Protein kinase activity associated with the large subunit of herpes simplex virus type 2 ribonucleotide reductase (ICP10). J. Virol. **63:**3389–3398.
8. **Cook, I. D., F. Shanahan, and P. J. Farell.** 1994. Epstein-Barr virus SM protein. Virology **205:**217–227.
9. **Daikoku, T., S. Shibata, S. Goshima, T. Tsurumi, H. Yamada, Y. Yamashita, and Y. Nishiyama.** 1997. Purification and characterization of the protein kinase encoded by the UL13 gene of herpes simplex virus type 2. Virology **235:**82–93.
10. **Daikoku, T., Y. Yamashita, T. Tsurumi, K. Maeno, and Y. Nishiyama.** 1993. Purification and biochemical characterization of the protein kinase encoded by the US3 gene of herpes simplex virus type 2. Virology **197:**685–694.
11. **Frame, M. C., F. Purves, D. J. McGeoch, H. S. Marsden, and D. P. Leader.** 1987. Identification of the herpes simplex virus protein kinase as the product of viral gene US3. J. Gen. Virol. **68:**2699–2704.
12. **Ghisolfi, L., G. Joseph, F. Amalric, and M. Erard.** 1992. The glycine-rich domain of nucleolin has an unusual supersecondary structure responsible for its RNA-helix-destabilizing properties. J. Biol. Chem. **267:**2955–2959.
13. **Hardwicke, M. A., and R. M. Sandri-Goldin.** 1994. The herpes simplex virus regulatory protein ICP27 contributes to the decrease in cellular mRNA levels during infection. J. Virol. **68:**4797–4810.
14. **Hardwicke, M. A., P. J. Vaughan, R. E. Sekulovich, R. O'Conner, and R. M. Sandri-Goldin.** 1989. The regions important for the activator and repressor functions of herpes simplex virus type 1 α protein ICP27 map to the C-terminal half of the molecule. J. Virol. **63:**4590–4602.
15. **Hardy, W. R., and R. M. Sandri-Goldin.** 1994. Herpes simplex virus inhibits host cell splicing, and regulatory protein ICP27 is required for this effect. J. Virol. **68:**7790–7799.
16. **Hibbard, M. K., and R. M. Sandri-Goldin.** 1995. Arginine-rich regions succeeding the nuclear localization region of the herpes simplex virus type 1 regulatory protein ICP27 are required for efficient nuclear localization and late gene expression. J. Virol. **69:**4656–4667.
17. **Hopp, T. P., K. S. Prickett, V. Price, R. T. Libby, C. J. March, P. Cerretti, D. L. Urdal, and P. J. Conlon.** 1988. A short polypeptide marker sequence useful for recombinant protein identification and purification. Bio/Technology **6:**1205–1210.
18. **Jans, D. A.** 1995. The regulation of protein transport to the nucleus by phosphorylation. Biochem. J. **311:**705–716.
19. **Jans, D. A., M. Ackermann, J. R. Bischoff, and D. H. Beach.** 1991. $p34^{cdc2}$-mediated phosphorylation at T^{124} inhibits nuclear import of SV40 T-antigen proteins. J. Cell Biol. **115:**1203–1212.
20. **Jans, D. A., and P. Jans.** 1994. Negative charge at the casein kinase II site flanking the nuclear localization signal of the SV40 large T-antigen is mechanistically important for enhanced nuclear import. Oncogene **9:**2961–2968.
21. **Kiledjian, M., and G. Dreyfuss.** 1992. Primary structure and binding activity of the hnRNP U protein: binding RNA through RGG box. EMBO J. **11:**2655–2664.
22. **Knipe, D. M., D. Senechek, S. A. Rice, and J. L. Smith.** 1987. Stages in the nuclear localization of the herpes simplex virus transcriptional activator protein ICP4. J. Virol. **61:**276–284.
23. **Liu, Q., and G. Dreyfuss.** 1995. In vivo and in vitro arginine methylation of RNA-binding proteins. Mol. Cell. Biol. **15:**2800–2808.
24. **McCarthy, A. M., L. McMahan, and P. A. Schaffer.** 1989. Herpes simplex virus type 1 ICP27 deletion mutants exhibit altered patterns of transcription and are DNA deficient. J. Virol. **63:**18–27.
25. **McGregor, F., A. Phelan, J. Dunlop, and J. B. Clements.** 1996. Regulation of herpes simplex virus poly(A) site usage and the action of immediate-early protein IE63 in the early-late switch. J. Virol. **70:**1931–1940.
26. **McLauchlan, J., A. Phelan, C. Loney, R. M. Sandri-Goldin, and J. B. Clements.** 1992. Herpes simplex virus IE63 acts at the posttranscriptional level to stimulate viral mRNA 3′ processing. J. Virol. **66:**6939–6945.
27. **McMahan, L., and P. A. Schaffer.** 1990. The repressing and enhancing functions of the herpes simplex virus regulatory protein ICP27 map to C-terminal regions and are required to modulate viral gene expression very early in infection. J. Virol. **64:**3471–3485.
28. **Mears, W. E., V. Lam, and S. A. Rice.** 1995. Identification of nuclear and nucleolar localization signals in the herpes simplex virus regulatory protein ICP27. J. Virol. **69:**935–947.
29. **Mears, W. E., and S. A. Rice.** 1996. The RGG box motif of the herpes simplex virus ICP27 protein mediates an RNA-binding activity and determines in vivo methylation. J. Virol. **70:**7445–7453.
30. **Mears, W. E., and S. A. Rice.** 1998. The herpes simplex virus immediate-early protein ICP27 shuttles between the nucleus and cytoplasm. Virology **242:**128–137.
31. **Panagiotidis, C. A., E. K. Lium, and S. J. Silverstein.** 1997. Physical and functional interactions between herpes simplex virus immediate-early proteins ICP4 and ICP27. J. Virol. **71:**1547–1557.
32. **Pearson, R. B., and B. E. Kemp.** 1991. Protein kinase phosphorylation site sequences and consensus specificity motifs: tabulations. Methods Enzymol. **200:**62–81.
33. **Pereira, L., M. H. Wolff, M. Fenwick, and B. Roizman.** 1977. Regulation of herpesvirus macromolecular synthesis. V. Properties of alpha polypeptides

made in HSV-1 and HSV-2 infected cells. Virology **77:**733–749.
34. **Phelan, A., M. Carmo-Fonseca, J. McLauchlan, A. I. Lamond, and J. B. Clements.** 1993. A herpes simplex virus type 1 immediate-early gene product, IE63, regulates small nuclear ribonucleoprotein distribution. Proc. Natl. Acad. Sci. USA **90:**9056–9060.
35. **Phelan, A., and J. B. Clements.** 1997. Herpes simplex virus type 1 immediate early protein IE63 shuttles between nuclear compartments and the cytoplasm. J. Gen. Virol. **78:**3327–3331.
36. **Phelan, A., J. Dunlop, and J. B. Clements.** 1996. Herpes simplex virus type 1 protein IE63 affects the nuclear export of virus intron-containing transcripts. J. Virol. **70:**5255–5265.
37. **Rice, S. A., and D. M. Knipe.** 1988. Gene-specific transactivation by herpes simplex virus type 1 alpha protein ICP27. J. Virol. **62:**3814–3823.
38. **Rice, S. A., and D. M. Knipe.** 1990. Genetic evidence for two distinct transactivation functions of the herpes simplex virus α protein ICP27. J. Virol. **64:** 1704–1715.
39. **Rice, S. A., V. Lam, and D. M. Knipe.** 1993. The acidic amino-terminal region of herpes simplex virus type 1 alpha protein ICP27 is required for an essential lytic function. J. Virol. **67:**1778–1787.
40. **Rice, S. A., L. Su, and D. M. Knipe.** 1989. Herpes simplex virus alpha protein ICP27 possesses separable positive and negative regulatory activities. J. Virol. **63:**3399–3407.
41. **Sacks, W. R., C. C. Greene, D. P. Aschman, and P. A. Schaffer.** 1985. Herpes simplex virus type 1 ICP27 is an essential regulatory protein. J. Virol. **55:**796–805.
42. **Sandri-Goldin, R. M.** 1998. ICP27 mediates herpes simplex virus RNA export by shuttling through a leucine-rich nuclear export signal and binding viral intronless RNAs through a RGG motif. Genes Dev. **12:**868–879.
43. **Sandri-Goldin, R. M., and M. K. Hibbard.** 1996. The herpes simplex virus type 1 regulatory protein ICP27 coimmunoprecipitates with anti-Sm antiserum, and the C terminus appears to be required for this interaction. J. Virol. **70:**108–118.
44. **Sandri-Goldin, R. M., M. K. Hibbard, and M. A. Hardwicke.** 1995. The C-terminal repressor region of herpes simplex virus type 1 ICP27 is required for the redistribution of small nuclear ribonucleoprotein particles and splicing factor SC35; however, these alterations are not sufficient to inhibit host cell splicing. J. Virol. **69:**6063–6076.
45. **Sandri-Goldin, R. M., and G. E. Mendoza.** 1992. A herpes virus regulatory protein appears to act posttranscriptionally by affecting mRNA processing. Genes Dev. **6:**848–863.
46. **Sekulovich, R. E., K. Leary, and R. M. Sandri-Goldin.** 1988. The herpes simplex virus type 1 α protein ICP27 can act as a *trans*-repressor or a *trans*-activator in combination with ICP4 and ICP0. J. Virol. **62:**4510–4522.
47. **Smith, I. L., M. A. Hardwicke, and R. M. Sandri-Goldin.** 1992. Evidence that the herpes simplex virus immediate early protein ICP27 acts posttranscriptionally during infection to regulate gene expression. Virology **186:**74–86.
48. **Smith, I. L., R. E. Sekulovich, M. A. Hardwicke, and R. M. Sandri-Goldin.** 1991. Mutations in the activation region of herpes simplex virus regulatory protein ICP27 can be *trans* dominant. J. Virol. **65:**3656–3666.
49. **Soliman, T. M., R. M. Sandri-Goldin, and S. J. Silverstein.** 1997. Shuttling of the herpes simplex virus type 1 regulatory protein ICP27 between the nucleus and cytoplasm mediates the expression of late proteins. J. Virol. **71:** 9188–9197.
50. **Wilcox, K. W., A. Kohn, E. Sklyanskaya, and B. Roizman.** 1980. Herpes simplex virus phosphoproteins. I. Phosphate cycles on and off some viral polypeptides and can alter their affinity for DNA. J. Virol. **33:**167–182.
51. **William, J. B., P. V. D. Geer, and T. Hunter.** 1991. Phosphopeptide mapping and phosphoamino acid analysis by two-dimensional separation on thin-layer cellulose plates. Methods Enzymol. **201:**111–149.
52. **Xia, K., N. A. DeLuca, and D. M. Knipe.** 1996. Analysis of phosphorylation sites of herpes simplex virus type 1 ICP4. J. Virol. **70:**1061–1071.
53. **Xia, K., D. M. Knipe, and N. A. DeLuca.** 1996. Role of protein kinase A and the serine-rich region of herpes simplex virus type 1 ICP4 in viral replication. J. Virol. **70:**1050–1060.
54. **Zhi, Y., C. Sciabica, and R. M. Sandri-Goldin.** Self-interaction of the herpes simplex virus type 1 regulatory protein ICP27. Virology, in press.
55. **Zhi, Y., and R. M. Sandri-Goldin.** Unpublished data.